PAPER

Cite this: DOI: 10.1039/d5fb00871a

Freezing as a structuring process for protein gels: process–structure relationship, material characterization, and comparison with meats

Israel Jovino Caneschi, [ID] *[a] Daniel Angelo Longhi, [ID] [b] Charles Windson Isidoro Haminiuk [ID] [c] and Maria Lucia Masson [ID] [a]

The growing demand for alternative proteins arises from population growth and the pursuit of innovative, sustainable products. Protein gels stand out among these alternatives due to their ability to replicate meat-like sensory properties using proteins such as Soy Protein Isolate (SPI). This study evaluated the production of structured SPI gels *via* freeze structuring. The variables solids content (X_1), pH (X_2), and freezing temperature (X_3) were analysed in relation to the responses hardness (Y_1) and cohesiveness (Y_2), using a two-level, three-factor full factorial design with a duplicate at the centre point. The results revealed a significant effect of all main effects and they include the interactions solids content × pH and solids content × freezing temperature for Y_1, while for Y_2, the influential effects were solids content, pH, and the interactions solids content × pH and pH × freezing temperature. The Texture Profile Analysis (TPA) and colour of the gels were comparable to those of sirloin steak, chicken breast, and fish fillet. Gels exhibited acidity between 0.079 and 0.167 g of lactic acid/100 g, pH from 5.54 to 6.54, a water activity (a_w) of 0.992 to 0.996, and a moisture content of 63.35% to 69.84%. Treatments S6 (13% solids, pH 5.0, −5 °C), S8 (13% solids, pH 6.0, −5 °C), and S9 (9% solids, pH 5.5, −10 °C) exhibited lamellar structures and a Degree of Texturization (DT) above 1, suggesting unidirectional freezing, confirmed by freezing curves. Overall, freeze structuring proved to be a promising technique for producing structured SPI gels, with optimal parameters being 9% solids, pH 5.5, and −10 °C.

Sustainability spotlight

The demand for affordable and high-quality products increases with global population growth; it can cause environmental impacts and raises ethical concerns. The use of plant proteins and the development of meat analogues represent environmentally friendly alternatives to livestock products. In this context, a protein gel was produced from soy protein isolate, a residual material recovered during legume processing. The process uses an innovative freeze alignment technique that promotes protein rearrangement and organization to achieve meat-like textures. Low freezing rates and limited material requirements enhance reproducibility and contribute to sustainability, in accordance with Sustainable Development Goals 2, 9, and 13.

1. Introduction

The accelerated growth of the global population, concerns about animal welfare, and the environmental impact caused by livestock production, particularly regarding the exploitation of natural resources such as water and soil and the emission of greenhouse gases,[1–4] have influenced consumers to reduce or eliminate meat consumption. Consequently, the demand for

[a] Postgraduate Program in Food Engineering, Federal University of Paraná (UFPR), Polytechnic Centre, Curitiba, Paraná, CEP 81531-980, Brazil. E-mail: israeljcaneschi@gmail.com

[b] Postgraduate Program in Food Engineering, Federal University of Paraná (UFPR), Jandaia do Sul Campus, Jandaia do Sul, Paraná, CEP 86900-000, Brazil

[c] Postgraduate Program in Food Engineering, Biotechnology Laboratory, Federal Technological University of Paraná (UTFPR), Curitiba, Paraná, CEP 81280-340, Brazil

alternative and more sustainable protein sources has increased, driving the development of plant-based products.

Among the available plant sources, soybean stands out due to its wide availability, low cost, and high protein functionality, presenting properties such as solubility, emulsification, and gelation.[5] Preece *et al.*[6] explained that their protein derivatives (soy flour, concentrates, and isolates) are often obtained as co-products from oil extraction and exhibit great potential for the development of textured protein materials.[7–9]

Meat is a complex raw material composed of aligned myofibrils forming fibres, which are organised into muscles.[10] This assembly provides meat with its typical structural anisotropy, a fundamental aspect when attempting to reproduce its texture. To replicate this fibrous morphology in meat analogues, several structuring technologies have been proposed and developed. Among these, the freeze alignment technique stands

out for enabling control of the protein orientation during processing. This method is based on the freezing of a binary solution of water and biopolymers, resulting in the formation of plate-shaped ice crystals that promote the alignment and reorganisation of soybean globular proteins, generating a porous and fibrous structure similar to that of muscle tissue. Heat removal must occur unidirectionally to ensure the formation of the desired anisotropic structure.[11,12] Despite previous reports on the use of freeze alignment for protein structuring, its application under simplified freezing conditions and using low-complexity formulations remains insufficiently explored.

Given that the performance of the freeze alignment process directly influences product quality, it is essential to parameterise its stages to ensure the desired properties and reproducibility. For this purpose, experimental methodologies allow the simultaneous evaluation of the effects of different factors on parameters of interest. The Full Factorial Design (FFD) is a simple and efficient approach capable of identifying the factors that affect material formation and statistically analysing interactions between multiple parameters within a specific range of values.[13,14] In this study, texture was adopted as the response variable, as it represents a key property both for the development of novel food materials and for quality control during production, being one of the main characteristics to be controlled in structured products. According to Di Monaco et al.,[15] the study of texture involves the analysis of the mechanical properties of the material, which can be determined by different instrumental methods.

This study investigates the effect of process variables on quality parameters of meat analogue, plant-based gels. The use of formulations composed exclusively of plant protein and a gelling agent, in combination with freezing performed in a single step in a domestic freezer suggests that a cost-effective meat analogue could be obtained. The present work contributes to the United Nations Sustainable Development Goals[16] by proposing the use of freeze alignment technology in the production of meat analogues based on soy protein isolate, promoting access to sustainable protein sources and responsible production. Therefore, the aim of this study was to evaluate the effect of solids content, pH, and freezing temperature on the texture of the resulting protein gels. The physicochemical properties of the product were also examined, enabling its characterisation in terms of quality and preservation capacity, as well as the comparison of its texture and colour with those of conventional meats.

2. Materials and methods

2.1. Materials

For the development of this study, Soy Protein Isolate (SPI) donated by the company International Flavors & Fragrances – IFF was used. Its composition on a wet basis was 6.16% moisture, 4.65% ash, 0.19% lipids, 79.13% protein, and 9.87% carbohydrates, along with a solubility in water of 8.88%. Sodium alginate PA (SA) and calcium chloride PA (CaCl$_2$) were acquired from Êxodo Científica, and lactic acid (85%) from Nuclear. Cylindrical moulds made of expanded polystyrene with

dimensions of 110 × 68 × 82 mm (height, internal diameter, and external diameter, respectively) were also used.

2.2. Methods

2.2.1. Preparation of the protein gels. The formulation for obtaining the protein gel was prepared based on the modified methodology of Masson et al.,[17] with the addition of SA to the formulation. The SPI was first hydrated in a 10% (w/v) dispersion, stirred for 2 hours at room temperature, and then placed in a refrigerated water bath at 4 °C for 12 hours. Subsequently, the dispersion underwent coagulation using a saline solution (5% CaCl$_2$) and was heated in a water bath at 90 °C for 2 hours. The material obtained from this step was drained and incorporated into the formulation, in which sodium alginate was added in a 9.5 : 0.5 ratio (SPI : SA), along with water, and the pH was adjusted by adding lactic acid. The formulated product was then transferred to expanded polystyrene moulds and subjected to freezing for 36 hours in a freezer (Electrolux PROSDOCIMO H40C). Following freezing, the samples were stabilized with steam in an autoclave (HOENIX brand), operating at 137.29 kPa, cooled to room temperature (20 °C), and subsequently prepared for the relevant analyses.

2.2.2. Chemical and physical properties of texturisers. The protein content and total titratable acidity were determined according to the Association of Official Analytical Chemists – AOAC,[18] using the Kjeldahl method (991.20) with a nitrogen-to-protein conversion factor of N × 6.25, and potentiometric volumetry (942.15 B), respectively. The pH of the samples was measured by the potentiometric method using a digital pH meter, in a 10% (w/v) dispersion of ground analogue in deionised water. Moisture content was determined by infrared drying using an IVT 200 analyser (Gehaka), and water activity was measured directly using an AquaLab device, Series 3 TE model.

2.2.3. Colour. Colour measurements were performed using a MiniScan XE Plus colorimeter (HunterLab). Colour evaluation (CIE L*a*b* scale) was conducted on different surface points of the sample. In addition, chroma (C*) and hue angle (h°) values were calculated according to eqn (1) and (2), respectively. The total colour difference (ΔE*) was calculated in comparison with meat products, based on eqn (3). The D65 illuminant and the 10 degree angle for the observer were used. The colour analysis methodology followed the approach described by Pathare et al.[19]

$$C^* = \sqrt{a^{*2} + b^{*2}} \tag{1}$$

$$h° = \tan^{-1}\left(\frac{b^*}{a^*}\right) \tag{2}$$

$$\Delta E^* = \sqrt{(\Delta L^*)^2 + (\Delta a^*)^2 + (\Delta b^*)^2} \tag{3}$$

2.2.4. Texture. Texture Profile Analysis (TPA) was conducted following the methodology described by Wagner et al.[20] and Yuliarti et al.,[12] with minor modifications. Each sample underwent two consecutive compressions, and the test was performed in triplicate. The compression parameters were set as follows:

Paper

Sustainable Food Technology

pre-test speed of 1.0 mm s^{-1}, test speed of 2.0 mm s^{-1}, and post-test speed of 2.0 mm s^{-1}. Compression was set to 30% of the sample's original height, utilising a 38 mm diameter cylindrical probe. Hardness, springiness, cohesiveness, and chewiness of the produced analogue were determined using a BROOKFIELD CT3 25K texture analyser, equipped with a 245 N load cell.

2.2.5. Meat preparation. Chicken breast, panga fish fillet, and beef sirloin were used as comparative samples for the products developed in this study. Chicken breast and fish fillet were cut into 40 × 40 × 20 mm pieces and cooked in an autoclave for 35 minutes. The beef sirloin, on the other hand, was sliced into 25 mm thick steaks and grilled over medium heat for 2.5 minutes per side, which is sufficient to achieve the ideal doneness for barbecue consumption in Brazil. After preparation, the samples were left to rest until they reached room temperature (20 °C), before being subjected to TPA following the same procedure described in Section 2.2.4 (Texture).

2.2.6. Visible appearance. Samples were sectioned longitudinally to expose their internal structure. Images were then captured using a digital camera, as performed by Singh et al.[3] The sample was cut in half and further sectioned into pieces measuring 10 × 10 mm, rapidly frozen using liquid nitrogen, and then freeze-dried. The dried material's macrostructure was then observed under a Bioptika 5MP magnifying glass, available at the Wood Anatomy Laboratory, Department of Forest Engineering, Federal University of Paraná (UFPR). To enhance observation, 2× magnifying lenses were used, allowing for greater clarity in the analysis.

2.2.7. Scanning electron microscopy (SEM). Scanning Electron Microscopy (SEM) was performed according to Yuliarti et al.,[21] with minor modifications. The analyses were conducted using a Zeiss scanning electron microscope (model EVO MA 15), available at the Multi-user Centre for Materials Characterisation (CMCM) of the Federal Technological University of Paraná (UTFPR). Sample preparation was similar to that performed for the magnifying glass analyses, with the material being gold-coated after freeze-drying.

2.2.8. Freezing temperature profiles. The temperature profile was obtained following the procedure described by Jie et al.[22] PT-100 sensors were used and positioned at five different points in the sample. Three sensors were vertically aligned in the centre of the sample, with 30 mm spacing between the lower point (Point 1), the centre point (Point 2), and the upper point (Point 3). Two additional sensors (Points 4 and 5) were positioned horizontally relative to the lower point, located near the base of the mould and spaced 20 mm apart. Temperature readings were recorded using a Novus – LogBoxble device at regular intervals of 60 seconds and were concluded at the end of the freezing process.

2.2.9. Degree of texturization (DT). The DT was determined according to Chen et al.,[23] with some modifications. The samples, cooled to room temperature (20 °C), were cut using a cylindrical knife with a 12.5 mm diameter. Using a TA7 probe, the samples were cut to 75% of their original thickness at a speed of 1 mm s^{-1}. The test was repeated at least 10 times, in both the vertical (F_V) and transverse (F_L) directions relative to the fibre length. The DT was calculated as the ratio of F_V to F_L.

2.2.10. Experimental design. The OriginPro[24] software was employed to systematically investigate three process variables: solids content (X_1), pH (X_2), and freezing temperature (X_3). These parameters were evaluated for their influence on texture properties of hardness (Y_1) and cohesiveness (Y_2). Thus, a two-level, three-factor (2^3) full factorial design, with duplicates at the centre point (Table 1), was utilised to identify experimental variables and interactions significantly influencing the production of textured soy protein using freezing.

The responses obtained were determined experimentally, and the first-order equation presented in eqn (4) was fitted to the experimental data to estimate its coefficients.

$$Y = \beta_0 + \sum_{i=1}^{n} \beta_i X_i + \sum \sum_{j < i} \beta_{ij} X_i X_j + \varepsilon \tag{4}$$

where X corresponds to the controllable process variables (in coded units), Y corresponds to the studied response variables, β_0 is the constant coefficient, n is the number of factors, β_i represents the coefficients of the linear parameters, β_{ij} represents the coefficients of the interaction parameters, and ε is the error term.

Table 1 Full factorial design 2^3 with duplicates at the centre point, presented in standard order[a]

Standard order	Random order	Solids content (%) X_1	pH (—) X_2	Freezing temperature (°C) X_3	Hardness (N) Y_1	Cohesiveness (—) Y_2
1	8	5 (−1)	5 (−1)	−15 (−1)	81.62 ± 2.30	0.65 ± 0.01
2	2	13 (1)	5 (−1)	−15 (−1)	83.76 ± 2.19	0.63 ± 0.02
3	3	5 (−1)	6 (1)	−15 (−1)	50.26 ± 0.52	0.70 ± 0.01
4	5	13 (1)	6 (1)	−15 (−1)	98.45 ± 1.06	0.64 ± 0.01
5	9	5 (−1)	5 (−1)	−5 (1)	74.94 ± 1.93	0.62 ± 0.01
6	10	13 (1)	5 (−1)	−5 (1)	125.42 ± 8.12	0.63 ± 0.03
7	1	5 (−1)	6 (1)	−5 (1)	44.65 ± 2.73	0.71 ± 0.04
8	4	13 (1)	6 (1)	−5 (1)	127.16 ± 3.12	0.68 ± 0.01
9	7	9 (0)	5.5 (0)	−10 (0)	93.06 ± 2.06	0.66 ± 0.02
10	6	9 (0)	5.5 (0)	−10 (0)	91.86 ± 4.88	0.67 ± 0.02

[a] The results are presented as mean ± standard deviation (SD), based on three replicates. The statistical significance of the terms used to derive mathematical models (presented in Section 3.6) was evaluated using the Student's t-test at a 95% confidence level (α = 0.05).

Process variables and their levels were established based on preliminary studies and the literature: X_1 – solids content (5% and 13%); X_2 – pH (5.0 and 6.0); and X_3 – freezing temperature (−15 °C and −5 °C). The selection of X_1 considered processing feasibility, as higher concentrations hindered homogenization and pH adjustment. For X_2, the range sought to align with typical values for red meat and poultry (5.5 to 5.9)[25] and Brazilian freshness standards for fish (pH < 7.0), according to national legislation.[26] Freezing temperatures (X_3) were set to ensure a slow-freezing regime, accounting for the small sample dimensions and similar meat analogue studies.[8,17] The centre point was defined at 9%, 5.5, and −10 °C, and the full factorial design comprised 10 randomized treatments to eliminate potential bias.[27] Statistical analysis was conducted at a 95% confidence level ($p < 0.05$), employing linear regression and ANOVA to assess main and secondary effects.

Non-significant interactions were removed, and the model was re-tested. Once the model proved adequate based on R^2 and adjusted R^2, it was established and presented in this work.

2.2.11. Statistical analysis. Statistical analyses were performed using ANOVA, followed by the Tukey's test at a 95% confidence level, for the comparison of means.

3. Results and discussion

3.1. Colour and texture characteristics in relation to meat standards

The Texture Profile Analysis (TPA) results for the protein gels and the three reference meats are presented in Table 2. According to Jonkers et al.,[28] hardness is directly related to a material's resistance to deformation, serving as an indicator of toughness and maturity in meat products. In this study, the treatments resulted in products with hardness ranging from 44.65 N (S7) to 127.16 N (S8), and Tukey's test was applied to compare these values with those of the reference meat products. Among the evaluated meats, the fish fillet showed the lowest hardness (24.04 N), differing significantly from all treatments.

Chicken breast (71.41 N) was statistically similar to samples S5 (74.94 N), S1 (81.62 N), and S2 (83.76 N), while beef striploin (54.17 N) was equivalent to S3 (50.26 N) and S7 (44.65 N). These findings support the model generated by the factorial design, which showed that samples with lower solids content, such as S1, S5, S3, and S7, yielded softer textures. In this regard, samples S8 and S6, which were prepared with a higher solids content and at a higher freezing temperature, exhibited the highest hardness among the treatments, differentiating them from the evaluated meat products. Furthermore, materials with a high gelling capacity tend to exhibit greater hardness, as is the case with SPI. Chantanuson et al.[8] demonstrated in their studies that hardness is influenced by both the solids content and the gelling capacity of the soy protein. They also explained that this capacity is directly related to the solubility of the raw material: the higher the solubility, the greater the gelling capacity. Thus, considering that the solubility obtained for the SPI used in this study was 8.88%, a high value compared to the results obtained by Chantanuson et al.,[7] it is believed that the gelling property contributed to the increased hardness of the resulting product.

Springiness results showed no significant differences among treatments at the 5% level, with values ranging from 0.83 (S1) to 0.90 (S8). All samples had elasticity values comparable to fish fillet (0.83) but differed significantly from those of striploin (0.72) and chicken breast (0.43). These values suggest that the material tends to break into larger fragments upon compression.[29]

Cohesiveness reflects the internal bonding of the material and indicates its structural integrity under mechanical stress.[30] High cohesiveness values imply stronger intermolecular forces and a more crosslinked structure.[31] Among the meat products, chicken breast (0.24) differed significantly from all treatments. Fish fillet (0.63) differed only from S7 (0.71) and S3 (0.70), while striploin (0.55) was statistically similar to S5 (0.62). In general, the samples showed higher cohesiveness than chicken breast and striploin, indicating a highly crosslinked structure.

Table 2 Results obtained for the comparison between texture properties and different types of meat[a]

Standard order	Hardness (N)	Cohesiveness	Springiness	Chewiness (N)
1	81.62 ± 2.30[CD]	0.65 ± 0.01[ABC]	0.83 ± 0.00[A]	44.02 ± 0.85[EF]
2	83.76 ± 2.19[CD]	0.63 ± 0.02[C]	0.88 ± 0.03[A]	46.76 ± 1.44[DE]
3	50.26 ± 0.52[E]	0.70 ± 0.01[AB]	0.88 ± 0.03[A]	31.35 ± 1.09[G]
4	98.45 ± 1.06[B]	0.64 ± 0.01[BC]	0.85 ± 0.02[A]	53.58 ± 1.71[C]
5	74.94 ± 1.93[D]	0.62 ± 0.01[CD]	0.84 ± 0.01[A]	38.72 ± 1.98[F]
6	125.42 ± 8.12[A]	0.63 ± 0.03[C]	0.86 ± 0.02[A]	67.26 ± 5.88[B]
7	44.65 ± 2.73[E]	0.71 ± 0.04[A]	0.86 ± 0.06[A]	27.38 ± 1.83[GH]
8	127.16 ± 3.12[A]	0.68 ± 0.01[ABC]	0.90 ± 0.03[A]	77.63 ± 0.19[A]
9	93.06 ± 2.06[BC]	0.66 ± 0.02[ABC]	0.90 ± 0.01[A]	55.64 ± 1.38[C]
10	91.86 ± 4.88[BC]	0.67 ± 0.02[ACB]	0.85 ± 0.02[A]	52.34 ± 1.32[CD]
Chicken breast	71.41 ± 5.80[D]	0.24 ± 0.03[E]	0.43 ± 0.03[C]	7.54 ± 0.57[I]
Fish fillet	24.04 ± 1.35[F]	0.63 ± 0.01[C]	0.83 ± 0.04[A]	12.54 ± 0.08[I]
Beef sirloin	54.17 ± 9.22[E]	0.55 ± 0.01[D]	0.72 ± 0.01[B]	21.46 ± 3.39[H]

[a] The results are presented as mean ± standard deviation (SD), based on three replicates. Means followed by different letters indicate statistically significant differences ($p < 0.05$) within the same column for each evaluated parameter. The trials were numbered from 1 to 10, with the combination of factors (solids content (X_1) in %; pH (X_2); freezing temperature (X_3) in °C) for each one being as follows: S1 (5; 5.0; −15), S2 (13; 5.0; −15), S3 (5; 6.0; −15), S4 (13; 6.0; −15), S5 (5; 5.0; −5), S6 (13; 5.0; −5), S7 (5; 6.0; −5), S8 (13; 6.0; −5), S9 (9; 5.5; −10), and S10 (9; 5.5; −10).

Chewiness values were higher in all samples compared to fish fillet (12.54 N) and chicken breast (7.54 N), reaching 77.63 N in sample S8. Striploin (21.47 N) was statistically similar to S7 (27.38 N), which had the lowest chewiness among the treatments. Since chewiness reflects the combined effects of hardness, cohesiveness, and elasticity, these results highlight the strong intermolecular interactions and brittle characteristics of the gels. According to Godschalk-Broers; Sala; Scholten,[32] chewiness is directly related to the effort required for mastication. Therefore, the high values indicate that the products analysed in this study offer greater resistance to chewing, requiring more effort to consume compared to the reference meat products.

Soy-based analogues produced by Chiang et al.[9] using wheat gluten and high-moisture extrusion had hardness values ranging from 45.40 N to 78.61 N, and chewiness values between 34.02 N and 45.32 N. Another study employing soy and rice protein with low-moisture extrusion reported elasticity values between 0.914 and 0.959 and cohesiveness ranging from 0.466 to 0.539.[29] These comparisons demonstrate that the textural properties observed in this study are similar to those found in previous research, reinforcing the influence of processing conditions and formulation on the final structure of meat analogues.

The texture results obtained in this study point to opportunities for improving the formulation and the resulting structure. Increasing the SA : SPI ratio and incorporating oil into the formulation may help enhance texture and bring it closer to that of conventional meat products. According to Nakagawa et al.,[4] enhancing protein–water interactions and adding lipids can promote the development of fibrous textures and improve product appearance. These improvements can be achieved using plant-based polysaccharides such as sugars, fibres, and starch.

Colour measurements are shown in Fig. 1 and Table S1 in the SI. Mean lightness (L^*) values for the treatments ranged from 54.03 (S8) to 68.83 (S5), classifying the samples as light ($L^* > 50$) and indicating higher light reflectance. The a^* coordinate (representing the red-green axis) varied between 4.37 (S3) and 5.84 (S4), while the b^* coordinate (yellow-blue axis) ranged from 19.18 (S3) to 21.95 (S1), suggesting that the samples displayed colours within the yellow to red spectrum. In a study conducted by Boonarsa et al.,[33] soy protein was used as a reference, and their reported values were $L^* = 74.64$, $a^* = 1.18$, and $b^* = 16.74$, also indicating light tones in the yellow-red region. The obtained C^* (chroma) ranged from 19.72 (S3) to 22.61 (S1), while $h°$ (hue angle) varied between 74.51° (S10) and 76.34° (S7), indicating a low-intensity colour closer to yellow.[19]

To assess the similarity or difference between the colour of the samples and that of meat products, the total colour difference (ΔE^*) was calculated and is presented in Table 3. Notable colour differences were observed between the grilled beef striploin and the treatments, reflecting both differences in red meat composition and preparation methods. As expected, the ΔE values were high when compared to beef, ranging from 21.31 (S8) to 35.57 (S5). The fish fillet and chicken breast presented lower ΔE values, indicating greater colour similarity with certain samples. Sample S6 exhibited the lowest variation compared to fish ($\Delta E^* = 6.12$), while for chicken breast the smallest difference was observed for sample S5 ($\Delta E^* = 3.86$).

Colour is a crucial parameter for product acceptance and is directly influenced by composition. Studies by Chiang et al.[9] and Lee et al.[34] showed that soy-based meat analogues exhibited colour variation when blended with other protein sources, such as wheat gluten and rice protein isolate, respectively. Furthermore, Chantanuson et al.[8] employed food colourants, such as Red 102, to achieve a reddish hue similar to raw meat. Thus, soy as a raw material offers broad potential for targeted modifications, due to its naturally light colour between red and yellow, which facilitates approximating the desired colour attributes in meat-like products. Differences in composition between meat products and analogues contribute to the variations observed in this study. Singh et al.,[3] in optimising the use of Manila tamarind protein isolate for meat analogue preparation, highlighted that colour differences in comparison with chicken breast were mainly due to compositional differences, since the latter has a higher fat content and lower carbohydrate concentration.

The differences observed in colour parameters (L^*, a^*, b^*) and texture (TPA) between the developed gels and the meats used as references should be interpreted considering the different cooking methods applied. The cooking method, which differs in terms of the heat transfer medium, processing time and applied temperature, directly influences muscle protein transformations and water redistribution within the matrix, thereby affecting the evaluated parameters.[35,36] Cooking temperature and time influence the extent of protein denaturation, muscle fibre contraction and water loss,[37] impacting colour attributes and the mechanical properties analysed. In addition, grilling, in which heating occurs more rapidly and is concentrated at the surface, promotes greater surface dehydration and intensifies non-enzymatic browning reactions, for example, affecting the final colour of the meat.[38] Thus, part of the variations observed in colour and texture results may be
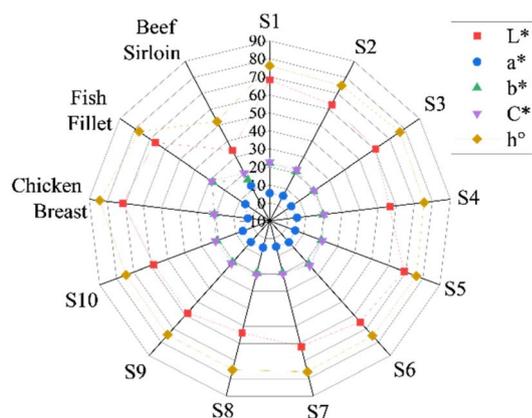

Fig. 1 Radar chart showing the variation of colour parameters in conventional meats and the study samples (S1–S10), which resulted from trials conducted using the combination of factors (solids content (X_1), pH (X_2), and freezing temperature (X_3)): S1 (5; 5.0; −15), S2 (13; 5.0; −15), S3 (5; 6.0; −15), S4 (13; 6.0; −15), S5 (5; 5.0; −5), S6 (13; 5.0; −5), S7 (5; 6.0; −5), S8 (13; 6.0; −5), S9 (9; 5.5; −10) and S10 (9; 5.5; −10).

Table 3 Colour variation results between samples and meats[a]

Standard order	ΔE^* – chicken breast	ΔE^* – fish fillet	ΔE^* – beef sirloin
1	4.59 ± 0.21^{FF}	6.44 ± 0.29^{F}	35.34 ± 0.34^{A}
2	9.15 ± 0.40^{DE}	7.79 ± 0.33^{E}	29.88 ± 0.43^{C}
3	11.19 ± 1.47^{C}	11.27 ± 0.58^{C}	27.56 ± 1.48^{D}
4	15.41 ± 1.22^{B}	13.56 ± 0.90^{B}	23.39 ± 1.19^{E}
5	3.86 ± 0.42^{F}	8.14 ± 0.34^{E}	35.57 ± 0.56^{A}
6	7.69 ± 0.69^{E}	6.12 ± 0.23^{F}	31.84 ± 0.73^{B}
7	10.02 ± 0.28^{CD}	9.99 ± 0.38^{D}	28.69 ± 0.28^{CD}
8	17.61 ± 0.58^{A}	15.18 ± 0.41^{A}	21.31 ± 0.52^{F}
9	13.72 ± 0.77^{B}	11.26 ± 0.47^{C}	25.20 ± 0.61^{E}
10	13.73 ± 0.70^{B}	11.12 ± 0.48^{CD}	25.21 ± 0.64^{E}

[a] The results are presented as mean $\pm$ standard deviation (SD), based on four repetitions. Means followed by different letters within the same column for each evaluated parameter indicate statistically significant differences ($p < 0.05$). The trials were numbered from 1 to 10, with the combination of factors (solids content (X_1) in %; pH (X_2); freezing temperature (X_3) in °C) for each one being as follows: S1 (5; 5.0; −15), S2 (13; 5.0; −15), S3 (5; 6.0; −15), S4 (13; 6.0; −15), S5 (5; 5.0; −5), S6 (13; 5.0; −5), S7 (5; 6.0; −5), S8 (13; 6.0; −5), S9 (9; 5.5; −10), and S10 (9; 5.5; −10).

attributed not only to the intrinsic characteristics of the evaluated matrices, but also to differences in cooking time, temperature and method. Nevertheless, the results allow the developed gels to be positioned within the range of instrumental properties observed in processed meat products, reinforcing their suitability as meat analogues from a technological perspective.

3.2. Physicochemical characterization of the protein gels

To characterise the obtained product, analyses of titratable acidity, pH, water activity (a_w), moisture, and protein content were performed. The samples were labelled according to the standard order established in the full factorial design 2^3, ranging from S1 to S10. These results are expressed together with the mean comparison analysis using Tukey's test (Table 4).

The protein gels exhibited protein contents ranging between 23.78% (S7) and 32.92% (S8), with formulations containing lower solids content resulting in lower protein values. However, sample S2 showed a statistically equivalent result to the centre point replicates (S9 and S10), despite having the lowest solids content among them. pH did not demonstrate a significant

influence on the protein content, unlike temperature, which impacted the protein levels in formulations with higher solids content (9% and 13%). Under these conditions, samples subjected to lower freezing temperatures (−5 °C and −10 °C) showed higher protein content. This occurs because faster freezing, promoted by lower temperatures, favours the retention of suspended solids. Consequently, during the stabilisation step, there is a greater loss of solids, which affects the final protein content in the material.

The samples displayed titratable acidity ranging between 0.079 and 0.167 g of lactic acid/100 g of the sample. The ANOVA results indicated variation in acidity among the samples, distributed according to the pH adjustment performed during formulation. Therefore, it was expected that the results would be similar for samples adjusted to pH 6.0 (S3, S4, S7, and S8), for those adjusted to pH 5.5 (S9 and S10), and for those adjusted to pH 5.0 (S5, S6, S1, S2), with the highest means observed for samples adjusted to pH 5, where a larger volume of acid was added.

All samples presented an acidic pH, ranging between 5.54 (S6) and 6.54 (S3), with this value being higher than the target

Table 4 Moisture, a_w, acidity, pH and protein results for protein gels[a]

Standard order	Moisture (%)	a_w (—)	Acidity g/100 g lactic acid	pH (—)	Protein (%)
1	69.19 ± 1.73^{AB}	0.994 ± 0.00^{AB}	0.16 ± 0.00^{A}	5.66 ± 0.09^{C}	25.28 ± 0.02^{E}
2	65.61 ± 2.86^{BCD}	0.992 ± 0.00^{C}	0.15 ± 0.01^{A}	5.55 ± 0.01^{D}	27.78 ± 0.25^{CD}
3	69.53 ± 0.73^{AB}	0.996 ± 0.00^{A}	0.08 ± 0.00^{C}	6.54 ± 0.02^{A}	25.36 ± 0.56^{E}
4	64.35 ± 1.64^{CD}	0.993 ± 0.00^{BC}	0.10 ± 0.00^{C}	6.50 ± 0.02^{A}	29.49 ± 0.02^{B}
5	66.79 ± 1.64^{ABC}	0.995 ± 0.00^{AB}	0.17 ± 0.01^{A}	5.67 ± 0.07^{C}	27.33 ± 0.21^{D}
6	63.35 ± 1.85^{CD}	0.995 ± 0.00^{AB}	0.16 ± 0.01^{A}	5.54 ± 0.04^{D}	30.09 ± 0.19^{B}
7	70.74 ± 1.63^{A}	0.996 ± 0.00^{A}	0.08 ± 0.01^{C}	6.50 ± 0.04^{A}	23.78 ± 0.02^{F}
8	61.45 ± 2.46^{D}	0.996 ± 0.00^{A}	0.09 ± 0.00^{C}	6.46 ± 0.02^{A}	32.92 ± 0.12^{A}
9	65.88 ± 1.81^{BCD}	0.995 ± 0.00^{AB}	0.12 ± 0.01^{B}	6.32 ± 0.02^{B}	28.24 ± 0.05^{CD}
10	65.71 ± 1.49^{BCD}	0.996 ± 0.00^{A}	0.12 ± 0.01^{B}	6.33 ± 0.03^{B}	28.39 ± 0.27^{C}

[a] The results are expressed as mean $\pm$ standard deviation (SD), considering two repetitions for protein content, three for acidity and four for the other parameters. Different letters indicate statistically significant differences ($p < 0.05$) within the same column for each parameter. The trials were numbered from 1 to 10, with the combination of factors (solids content (X_1) in %; pH (X_2); freezing temperature (X_3) in °C) for each one being as follows: S1 (5; 5.0; −15), S2 (13; 5.0; −15), S3 (5; 6.0; −15), S4 (13; 6.0; −15), S5 (5; 5.0; −5), S6 (13; 5.0; −5), S7 (5; 6.0; −5), S8 (13; 6.0; −5), S9 (9; 5.5; −10), and S10 (9; 5.5; −10).

pH used in the formulation. Samples adjusted to pH 6.0 resulted in gels with higher pH (6.46–6.54) and lower acidity (0.08–0.10 g of lactic acid/100 g of sample), whereas those adjusted to pH 5.0 showed a lower final pH (5.54–5.67) and higher acidity (0.15–0.17 g of lactic acid/100 g of sample). Since pH indicates the acidity or alkalinity of the medium based on the concentration of hydrogen ions (H^+), these results converge with those found for total titratable acidity.

Regarding water activity (a_w), the results from the mean comparison test indicated a significant difference among samples, ranging between 0.992 and 0.996. This property is an important quality parameter for food and is related to its stability and safety for consumption. Analysing the degree of water interaction with other components of the food matrix, as well as its availability for reactions and microbial growth, allows for the evaluation of factors that directly influence its deterioration.[39] In this regard, foods with a water activity (a_w) below 0.85 are considered safe, as they do not favour the activity of pathogenic microorganisms and the production of mycotoxins by fungi.[40,41]

Finally, moisture content in the samples ranged between 63.35% and 69.84% (S6 and S7, respectively), showing significantly different means at a 5% significance level. Samples with lower solids content exhibited higher moisture, possibly due to a reduced proximity between protein molecules, which favours the formation of protein–water bonds, even with the high availability of free water indicated by the a_w values. These results might also be linked to the addition of SA to the formulation, given that carbohydrate polymers, such as alginates derived from seaweed, possess a high water-holding capacity, promoting water incorporation and reducing syneresis.[5] Soy protein has been used in various studies as a reference product. Boonarsa et al.[33] used freezing as a texturising technology for meat analogues based on silkworm pupae, and for samples containing only soy, the moisture content was 69.59%. Chiang et al.,[9] when using high-moisture extrusion to obtain analogue products, reported lower results of 58.01%, which was also less than that of cooked chicken used for comparison in their study.

The results obtained for acidity, water activity (a_w) and moisture content are typical of highly perishable products and must be carefully considered when selecting packaging systems and storage conditions. The adoption of preservation strategies widely employed in the food industry, such as refrigeration combined with appropriate packaging systems, including modified atmosphere packaging, has been reported as effective in reducing microbiological and oxidative spoilage in high-a_w products, thereby contributing to shelf-life extension without compromising product characteristics.[42] Physical processes aimed at partially reducing water activity, such as controlled dehydration, have also been applied as an alternative to limit the availability of free water and improve physicochemical stability during storage.[43] Additionally, adjustments to formulation and packaging systems, including the incorporation of compounds with antioxidant and antimicrobial activity directly into the food matrix or into active packaging systems, are described as complementary and effective strategies to retard oxidative reactions and microbial growth in highly perishable foods.[44,45] Overall, the combined application of these approaches indicates that, despite the high perishability, there are viable and sustainable technological pathways for the practical application and commercialisation of the developed gels, while maintaining physicochemical properties, protein content and pH comparable to those of conventional meat products.

3.3. Structure assessment

Structural characterisation was performed using analyses of both the moist sample, through digital photography, and the freeze-dried sample, using a magnifying lens and scanning electron microscopy (SEM). Based on the SEM images (Fig. 2), it was possible to examine the microstructure of the material, which revealed a porous morphology in all samples. This was a result of ice crystal formation during the freezing process. However, detailed analysis of this microstructure did not reveal any clear porosity pattern that would suggest specific directional crystal growth or significant differences between samples.

Images obtained with the stereomicroscope, shown in Fig. 3, demonstrated differences in the structures resulting from the various treatments. A porous appearance was again observed across all samples. Some treatments, such as S1, S2, S3, S4, and S5, resulted in smaller openings, whereas samples such as S6, S7, S8, and S9 exhibited slightly larger openings. The absence of lamellar structures may be explained by the cutting direction and magnification used. Nonetheless, there was a trend towards
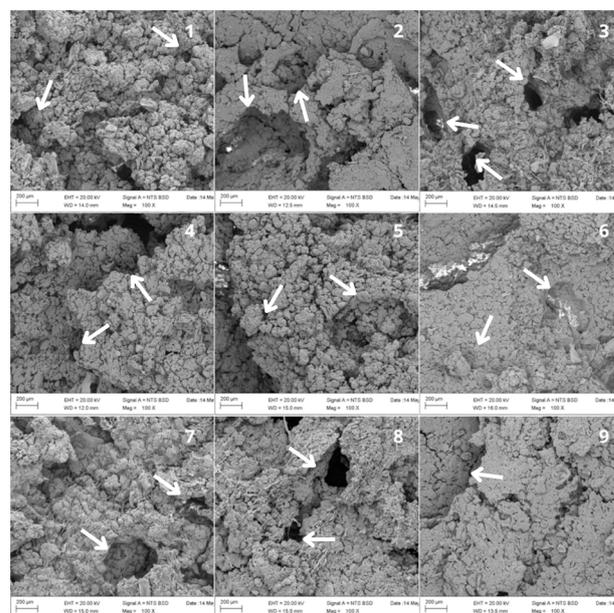

Fig. 2 Images obtained by Scanning Electron Microscopy (SEM) for the 9 treatments, numbered from 1 to 9, where each treatment corresponds to a combination of factors (solids content (X_1), pH (X_2), and freezing temperature (X_3)): S1 (5; 5.0; −15), S2 (13; 5.0; −15), S3 (5; 6.0; −15), S4 (13; 6.0; −15), S5 (5; 5.0; −5), S6 (13; 5.0; −5), S7 (5; 6.0; −5), S8 (13; 6.0; −5), and S9–S10 as a duplicate (9; 5.5; −10).
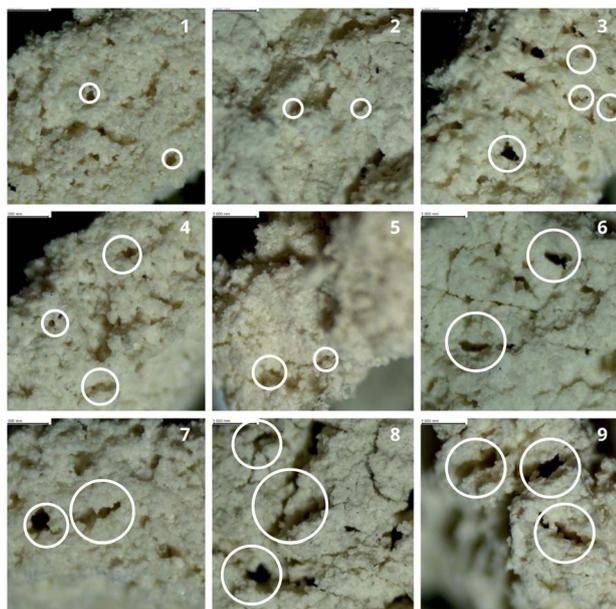
Fig. 3 Images obtained with a magnifying lens for the 9 treatments, numbered from 1 to 9, where each treatment corresponds to a combination of factors (solids content (X_1), pH (X_2), and freezing temperature (X_3)): S1 (5; 5.0; −15), S2 (13; 5.0; −15), S3 (5; 6.0; −15), S4 (13; 6.0; −15), S5 (5; 5.0; −5), S6 (13; 5.0; −5), S7 (5; 6.0; −5), S8 (13; 6.0; −5), and S9–S10 as a duplicate (9; 5.5; −10).

the formation of larger openings in treatments conducted at higher temperatures (−5 °C and −10 °C).

Images of the analogues, taken from longitudinal sections, allowed visualisation of the structure on a macroscopic scale

Fig. 4 Digital camera images for the 9 treatments, numbered from 1 to 9, where each treatment corresponds to a combination of factors (solids content (X_1), pH (X_2), and freezing temperature (X_3)): S1 (5; 5.0; −15), S2 (13; 5.0; −15), S3 (5; 6.0; −15), S4 (13; 6.0; −15), S5 (5; 5.0; −5), S6 (13; 5.0; −5), S7 (5; 6.0; −5), S8 (13; 6.0; −5), and S9–S10 as a duplicate (9; 5.5; −10).

(Fig. 4), essential for observing the lamellar morphology. Upon examining the images, it was evident that the structure differed between treatments, ranging from lamellar to porous forms. Samples S1 and S3 were predominantly porous. This outcome was associated with the formation of smaller ice crystals due to the lower processing temperature (−15 °C), combined with the lower solids content (5%). Samples S6, S8, and S9 exhibited predominantly lamellar structures, contrasting with the samples S6 and S8 which were prepared using 13% solids at −5 °C, while S9 was prepared under the central point conditions (9% solids and −10 °C). The combination of these processing parameters proved promising for the formation of the desired fibrous structure, showing better performance compared to the other treatments.

Samples S6, S8, and S9 showed the most promising results, taking into account the aim of the study. Although the macroscopic structure confirmed the formation of lamellar regions in these treatments, the images obtained using SEM and a stereoscope did not allow a definitive conclusion regarding the unidirectional orientation of ice crystal growth. This result stems from the orientation of the cut, made perpendicular to the growth plane of the leaves. Additionally, the high magnification used reduced the field of view, affecting the perception of the parallel arrangement of the layers.

3.4. Cutting force and degree of texturization (DT)

Samples S6, S8, and S9 were assessed for shear force in the vertical (F_V) and transverse (F_L) directions relative to the fibre orientation (Table S2 in the SI). The recorded ranges were: S6 (3.18–1.61 N), S8 (5.30–2.80 N), and S9 (5.71–2.12 N) in the vertical direction, and S6 (2.26–0.94 N), S8 (4.69–1.65 N), and S9 (4.79–1.12 N) in the transverse direction. These results indicated that sample S8 exhibited the highest resistance to shear, which is consistent with its hardness values, where it also recorded the highest result among the evaluated samples.

The ratio between the shear forces in the two directions was calculated to be 1.65 (S6), 1.67 (S8), and 1.45 (S9). According to Chen et al.,[23] this ratio serves as an indicator of the DT, with values greater than 1 suggesting the presence of fibrous structure formation. This is due to the higher resistance observed when fibres are aligned in parallel, compared to the perpendicular orientation. Thus, the results confirm the fibrous formation and anisotropic behaviour of the protein gels. Similar findings were reported by Chiang et al.,[9] Fang et al.[46] and Singh et al.,[3] showing degrees of texturization comparable to those observed in this study.

3.5. Freezing curve

The samples were frozen in cylindrical polystyrene moulds, insulated at the base and laterally. Five different points were monitored for temperature during the freezing process of the centre point samples (9% solids, pH 5.5 and temperature of −10 °C). The temperature profiles are shown in Fig. 5, which also identifies the respective locations of the sensors within the cylinder.
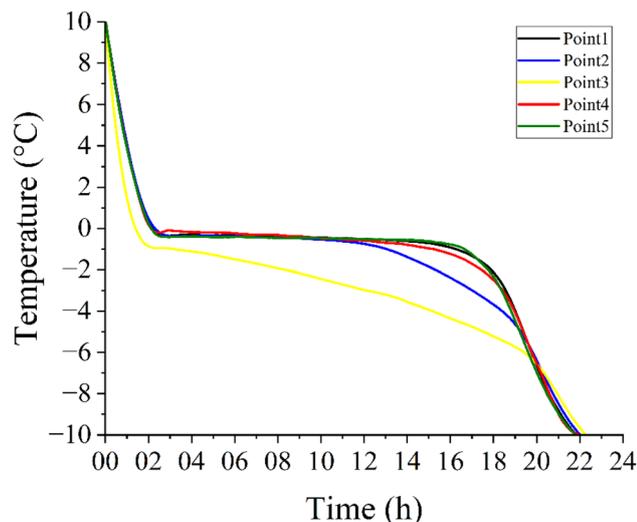
Fig. 5 Temperature profile at different points of the sample during the freezing process.

The freezing curves differed between Point 3 and the other measured points. This variation is attributed to the sample remaining static during freezing, which led to phase separation between the dispersed and continuous phases. The dispersed phase settled at the bottom of the cylinder, reaching Point 2, while the continuous phase was represented by Point 3. At this position, a marked depression in the freezing point and a wider ice crystal growth range (between -0.8 °C and -6.7 °C) were observed, indicating solute dissolution in water due to the colligative properties of solutions.[22,47]

Points 1, 2, 4, and 5 displayed similar behaviour, representing the freezing of the lower region of the sample where the dispersed solids accumulated. The separation between water and the solute initiated nucleation and ice crystal formation at freezing points close to that of pure water, ranging from 0 °C to -2 °C.[8,47,48] It was observed that heat loss predominantly occurred in the vertical direction, from bottom to top. Laterally, the temperature gradient was minimal, characterising unidirectional freezing of the material. Despite the insulating effect of the upper water layer, this freezing pattern was maintained.

3.6. Experimental design

3.6.1. Model significance. The results presented in Tables 5 and 6 correspond to the response variables hardness (Y_1) and cohesiveness (Y_2), obtained from fitting eqn (4) to the experimental data. Accordingly, the resulting models are described by using eqn (5) and (6).

$$Y_1 = 87.12 + 22.91X_1 - 5.65X_2 + 7.26X_3 + 19.52X_1X_2 + 20.67X_1X_3 \quad (5)$$

$$Y_2 = 0.659 - 0.014X_1 + 0.025X_2 - 0.012X_1X_2 + 0.021X_2X_3 \quad (6)$$

Based on the analysis of Table 5, considering a p-value lower than α (0.05), it was observed that the constant term (indicated

Table 5 Estimated coefficients of the model for the response hardness (Y_1)

	Effect	Value	Standard error	t-Value	Prob > $|t|$
(Intercept)		87.119	1.6898	51.5556	8.47×10^{-7}
X_1	45.8258	22.913	1.8893	12.1280	0.0003
X_2	-11.3025	-5.651	1.8893	-2.9913	0.0403
X_3	14.5208	7.260	1.8893	3.8430	0.0184
X_1X_2	19.5225	9.761	1.8893	5.1667	0.0067
X_1X_3	20.6658	10.333	1.8893	5.4693	0.0054
R^2	0.983				
Adj. R^2	0.961				

Table 6 Estimated coefficients of the model for the response cohesiveness (Y_2)

	Effect	Value	Standard error	t-Value	Prob > $|t|$
(Intercept)		0.659	0.0028	232.0052	1.77×10^{-7}
X_1	-0.029	-0.014	0.0032	-4.4861	0.0207
X_2	0.051	0.025	0.0032	7.9942	0.0041
X_3	0.001	0.001	0.0032	0.1700	0.8759
X_1X_2	-0.024	-0.012	0.0032	-3.7256	0.0337
X_1X_3	0.014	0.007	0.0032	2.1900	0.1163
X_2X_3	0.021	0.011	0.0032	3.3523	0.0440
R^2	0.974				
Adj. R^2	0.923				

in the table as the "intercept"), the main effects X_1, X_2 and X_3, as well as the interaction terms X_1X_2 and X_1X_3, exhibited significant coefficients and were statistically different from zero. In other words, these effects are associated with the response variable hardness (Y_1), as described by using eqn (5).

The same analytical procedure was applied to the response variable cohesiveness (Y_2), whose coefficients are presented in Table 6. In this case, the significant coefficients differed from those observed for Y_1. For Y_2, the constant term (intercept), the main effects X_1 and X_2, and the interaction terms X_1X_2 and X_2X_3 were significant at the 5% probability level ($p < 0.05$), being associated with the model described by using eqn (6). In contrast to the model obtained for hardness (Y_1), the coefficients X_3 and X_1X_3 were not significant and were therefore removed from the equation.

The Student's t-test can also be analysed using the t-critical value. The effects of the Y_1 and Y_2 models, respectively, were represented in the Pareto diagram (Fig. 6), in which they were ordered based on the degree of importance from the most significant to the least significant, as explained by Adio et al.[49]

In the graph, the critical line is represented by the dashed horizontal line in red. Effects that exceed the t-critical line are considered significant, while those that are within its limit were not significant for the model. Thus, the interpretations agree, indicating that the five effects shown in the diagram for hardness (Y_1) were significant, while X_3 and X_1X_3 were not significant for cohesiveness (Y_2).

In order to check the adequacy of the model, the R^2 and R^2aj. values were analysed, according to Nowalid et al.[50] and these
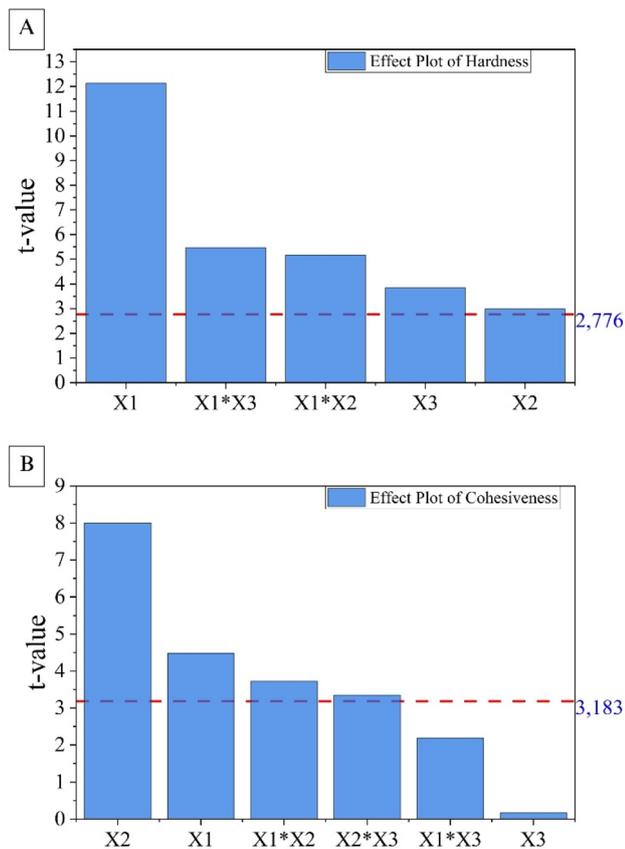
Fig. 6 Pareto chart showing the standardised effects from factorial analysis of (A) hardness (Y_1) and (B) cohesiveness (Y_2), considering solids content (X_1), pH (X_2) and freezing temperature (X_3).

Fig. 7 Main effect plots showing the influence of solids content (X_1), pH (X_2) and freezing temperature (X_3) on (A) hardness (Y_1) and (B) cohesiveness (Y_2).

values indicate how close the data are to the regression line. According to Karazhiyan *et al.*[51] models present good experimental fits for a minimum R^2 of 0.8. Rahmani *et al.*[52] indicated that higher values close to one for R^2 and the proximity between this value and that of R^2aj. suggest the high capacity of the fitted models. Thus, the equations generated for hardness (Y_1) and cohesiveness (Y_2) are well adjusted to the experimental data, as shown in Tables 5 and 6, indicating that the model has a good ability to describe the properties studied.

3.6.2. Main effects. Analysing the main effects within the factorial design is important in order to understand the key elements at one or more levels. The factors solids content (X_1), pH (X_2) and freezing temperature (X_3) are shown in Fig. 7 for each of the variables studied and are evaluated based on the slope of the line related to the level and the response of interest. Straight lines with lower or no slopes indicate a low effect of the variable on the response.

The results show that X_1, X_2 and X_3 have a significant influence on hardness (Y_1). In particular, X_1 and X_3 positively affect Y_1, so that an increase in the solids content or freezing temperature results in a higher hardness of the material. On the other hand, pH shows the opposite behaviour, indicating that when the formulation has a high pH, hardness tends to decrease.
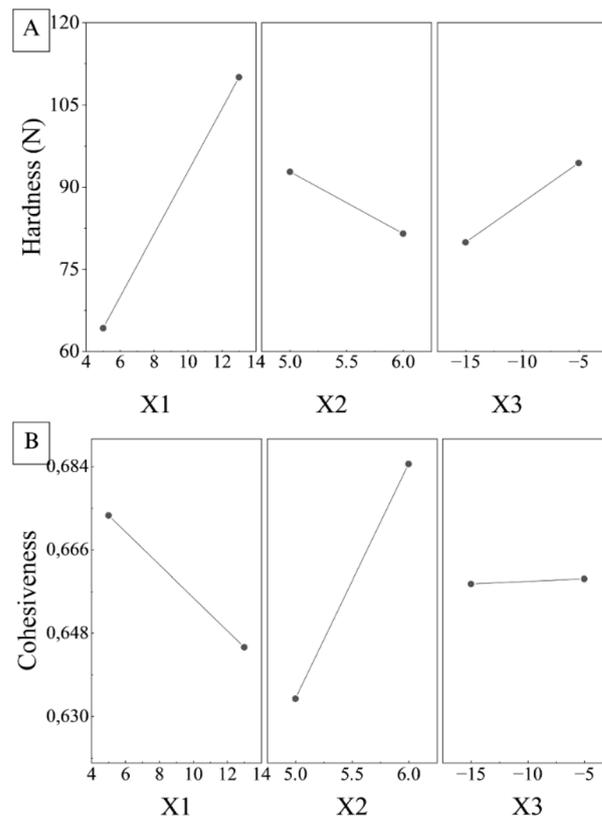
When evaluating these effects on cohesiveness (Y_2), this property is predominantly affected by pH, with higher values when the formulation has a higher pH. The solids content also has an influence, although inversely and with less impact compared to pH. Freezing temperature, on the other hand, has a minimal influence on the Y_2 response.

3.6.3. Interaction between effects. The interactions between the factors in a factorial design can enhance or reduce the main effects and are therefore important in the study.[14] For this investigation, the interaction graph was plotted (Fig. 8) representing the high (+1) and low (−1) levels of the parameters by the red and black colours respectively.

The graphs only show the interactions that showed statistical significance in the previous analysis. Thus, the X_2X_3 interaction is shown exclusively for cohesiveness (Y_2), since it was removed for hardness (Y_1) because it was not significant and impacted the main effects. According to Altayb *et al.*,[14] steep slopes suggest interaction between the factors analysed, which can be seen in Fig. 8. Both the X_2X_3 interaction for Y_2 and the X_1X_2 and X_1X_3 interactions for Y_1 and Y_2 are represented by lines with a clear slope, indicating interaction between the respective factors.

Based on Fig. 8, we can observe that hardness (Y_1), influenced by the X_1X_2 and X_1X_3 interactions, reached higher values at their respective high levels. In contrast, cohesiveness (Y_2) showed the opposite behavior, being lower at these same levels.
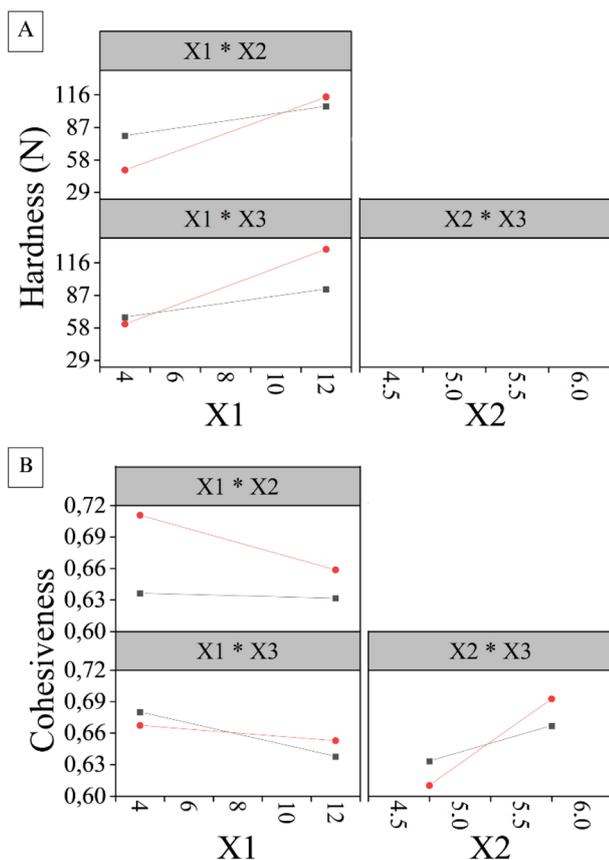
Fig. 8 Interaction effect plots showing the combined influence of solids content (X_1), pH (X_2) and freezing temperature (X_3) on (A) hardness (Y_1) and (B) cohesiveness (Y_2).

Additionally, it was found that high levels of the X_2X_3 interaction resulted in an increase in cohesiveness (Y_2) in the product.

3.6.4. Validation of the model. Parameters within the study range were established to validate the model. Although the centre point (0) was used in the experimental design, the positive (+0.5) and negative (−0.5) midpoints were studied for validation. Considering the positive midpoint (+0.5), the parameters were 11, 5.75 and −7.5, and for the negative midpoint (−0.5), 7, 5.25 and −12.5, for solids content (X_1), pH (X_2) and freezing temperature (X_3), respectively. Table 7 shows

Table 7 Validation of the models at the −0.5 and 0.5 levels[a]

Levels|parameters		−0.5		0.5
X_1 (%)		7		11
X_2		5.25		5.75
X_3 (°C)		−12.5		−7.5
Properties	T	E	T	E
Y_1 (N)	79.88	93.92	104.40	121.87
Y_2	0.66	0.73	0.67	0.75

[a] Solids content (X_1), pH (X_2), freezing temperature (X_3), hardness (Y_1), cohesiveness (Y_2), theoretical value (T) and experimental value (E).

the levels studied and the corresponding theoretical and experimental results obtained for each one. Based on these results, errors lower than 15% were observed for hardness (Y_1) and cohesiveness (Y_2), validating the model for this study.

4. Conclusions

Based on the full factorial design, it was observed that hardness (Y_1) was predominantly influenced by solids content (X_1), while cohesiveness (Y_2) was most significantly impacted by pH (X_2). The material demonstrated high potential for replicating the colour and texture of conventional meats, presenting values aligned with the literature and minimal colour differences compared to chicken breast and fish fillets. The freezing front suggests unidirectional crystal growth, while the DT indicated anisotropic behavior in samples S6 (13; 5.0; −5), S8 (13; 6.0; −5), and S9 (9; 5.5; −10), consistent with data described for protein gels. The centre point parameters (S9) yielded the best results regarding the formed structure and textural properties, indicating that the proposed methodology is promising for obtaining gels with meat-like properties. This study establishes a solid foundation in the field of alternative proteins, opening opportunities for further refinement through sensory studies, as well as the optimization of aspects related to the preservation and food safety of the developed products.

Author contributions

Israel Jovino Caneschi was responsible for the original draft preparation, data curation, formal analysis, investigation, methodology development, conceptualisation, and technical formatting. Daniel Angelo Longhi contributed to the formal analysis and data curation, and participated in the review and editing of the manuscript. Charles Windson Isidoro Haminiuk was responsible for data acquisition and language revision. Maria Lucia Masson contributed to data curation, methodology, and supervision, participated in the review and editing of the manuscript, and was responsible for funding acquisition.

Conflicts of interest

There are no conflicts to declare.

Data availability

Supplementary information (SI) is available. See DOI: https://doi.org/10.1039/d5fb00871a.

Acknowledgements

Characterisation (CMCM) – Federal Technological University of Paraná (UTFPR), and the Wood Anatomy Laboratory, Department of Forest Engineering – Federal University of Paraná (UFPR) for the infrastructure support.

References

1 U. Fresán, M. A. Mejia, W. J. Craig, K. Jaceldo-Siegl and J. Sabaté, *Sustainability*, 2019, **11**, 3231.

2 H. Aiking, *Trends Food Sci. Technol.*, 2011, **22**, 112–120.

3 A. Singh and N. Sit, *Int. J. Gastron. Food Sci.*, 2025, **39**, 101095.

4 K. Nakagawa, R. Chantanuson, P. Boonarsa, N. Seephua and S. Siriamornpun, *Food Chem.: X*, 2024, **22**, 101402.

5 L. Sha and Y. L. Xiong, *Trends Food Sci. Technol.*, 2020, **102**, 51–61.

6 K. E. Preece, N. Hooshyar and N. J. Zuidam, *Innovative Food Sci. Emerging Technol.*, 2017, **43**, 163–172.

7 R. Chantanuson, S. Nagamine, T. Kobayashi and K. Nakagawa, *J. Food Eng.*, 2024, **362**, 111779.

8 R. Chantanuson, S. Nagamine, T. Kobayashi and K. Nakagawa, *Food Struct.*, 2022, **32**, 100258.

9 J. H. Chiang, S. M. Loveday, A. K. Hardacre and M. E. Parker, *Food Struct.*, 2019, **19**, 100102.

10 G. Giménez-Ribes, M. Oostendorp, A. J. van der Goot, E. van der Linden and M. Habibi, *Food Hydrocolloids*, 2024, **149**, 109509.

11 O. K. Ozturk and B. R. Hamaker, *Future Foods*, 2023, **8**, 100248.

12 O. Yuliarti, T. J. Kiat Kovis and N. J. Yi, *J. Food Eng.*, 2021, **288**, 110138.

13 N. S. A. Mohd Sharif, M. F. Jamaluddin and N. Zainol, *Mater. Today: Proc.*, 2021, **46**, 1763–1769.

14 H. N. Altayb, B. Kouidhi, O. A. S. Baothman, J. A. Abdulhakim, L. Ayed, M. Hager and K. Chaieb, *J. Water Process Eng.*, 2021, **44**, 102429.

15 R. Di Monaco, S. Cavella and P. Masi, *J. Texture Stud.*, 2008, **39**, 129–149.

16 United Nations, *The 17 Goals*, https://sdgs.un.org/, accessed 21 October 2025.

17 M. L. Masson and H. A. Fugmann, *Bol. Cent. Pesqui. Process. Aliment.*, 1998, **16**, 189–202.

18 Association of Official Analytical Chemists (AOAC), *Official Methods of Analysis of the Association of Official Analytical Chemists*, Virgínia (USA), 16th edn, 1995.

19 P. B. Pathare, U. L. Opara and F. A.-J. Al-Said, *Food Bioprocess Technol.*, 2013, **6**, 36–60.

20 C. E. Wagner, L. Levine, S. R. Saunders, R. Bergman, X. Guo and G. M. Ganjyal, *Food Res. Int.*, 2024, **192**, 114760.

21 O. Yuliarti, K. H. Mei, Z. Kam Xue Ting and K. Y. Yi, *Food Hydrocolloids*, 2019, **89**, 216–223.

22 W. Jie, L. Lite and D. Yang, *J. Food Eng.*, 2003, **60**, 481–484.

23 F. L. Chen, Y. M. Wei, B. Zhang and A. O. Ojokoh, *J. Food Eng.*, 2010, **96**, 208–213.

24 *OriginPro, version 2025*, Northampton, MA, USA, 2025.

25 S. Damodaran and K. L. Parkin, *Química de alimentos de Fennema*, Artmed Editora Ltda, 5th edn, 2019.

26 P. e A. (MAPA) Ministério da Agricultura, *Instrução Normativa no. 21 de 31 de maio de 2017*, Brazil, 2017.

27 B. Gültekin Subaşı, B. Vahapoğlu, E. Capanoglu and M. A. Mohammadifar, *Crit. Rev. Food Sci. Nutr.*, 2021, **62**, 6682–6697.

28 N. Jonkers, J. A. W. van Dommelen and M. G. D. Geers, *Mech. Time-Depend. Mater.*, 2022, **26**, 323–346.

29 J.-S. Lee, H. Oh, I. Choi, C. S. Yoon and J. Han, *LWT*, 2022, **157**, 113056.

30 A. J. Rosenthal and P. Thompson, *J. Texture Stud.*, 2021, **52**, 294–302.

31 Y. Fan, S. Zheng, P. K. Annamalai, B. Bhandari and S. Prakash, *Sustainable Food Technol.*, 2024, **2**, 826–836.

32 L. Godschalk-Broers, G. Sala and E. Scholten, *Foods*, 2022, **11**, 2227.

33 P. Boonarsa, K. Nakagawa, K. Banlue and S. Siriamornpun, *Food Chem.: X*, 2025, **27**, 102370.

34 J.-S. Lee, I. Choi and J. Han, *Food Res. Int.*, 2022, **161**, 111840.

35 D. Barbanti and M. Pasquini, *LWT–Food Sci. Technol.*, 2005, **38**, 895–901.

36 J. Kim, Y. Zhang, Y. Han, Y. Lee, C. Kang, H. Jung and B.-J. Gu, *Food Sci. Preserv.*, 2025, **32**, 246–259.

37 B. I. Zielbauer, J. Franz, B. Viezens and T. A. Vilgis, *Food Biophys.*, 2016, **11**, 34–42.

38 J. Valentim, C. Afonso, R. Gomes, A. Gomes-Bispo, J. A. M. Prates, N. M. Bandarra and C. Cardoso, *Heliyon*, 2024, **10**, e27171.

39 E. P. Ribeiro and E. A. G. Seravalli, in *Química de alimentos*, Editora Blucher, 2nd edn, 2007, pp. 96–121.

40 L. R. Beuchat, E. Komitopoulou, H. Beckers, R. P. Betts, F. Bourdichon, S. Fanning, H. M. Joosten and B. H. Ter Kuile, *J. Food Prot.*, 2013, **76**, 150–172.

41 M. H. Taylor and M.-J. Zhu, *Trends Food Sci. Technol.*, 2021, **116**, 802–814.

42 U. Habiba, A. Bajpai, Z. Shafi, V. K. Pandey and R. Singh, *J. Stored Prod. Res.*, 2025, **112**, 102657.

43 D. Alp and Ö. Bulantekin, *Eur. Food Res. Technol.*, 2021, **247**, 1333–1343.

44 E. Zang, L. Jiang, H. Cui, X. Li, Y. Yan, Q. Liu, Z. Chen and M. Li, *Food Rev. Int.*, 2023, **39**, 5132–5163.

45 A. Kumar, S. Das, S. Ali, S. G. Jaiswal, A. Rabbani, S. M. E. Rahman, R. Chelliah, D.-H. Oh, S. Liu and S. Wei, *Food Biosci.*, 2025, **74**, 107864.

46 Y. Fang, B. Zhang and Y. Wei, *J. Food Eng.*, 2014, **121**, 32–38.

47 A. L. de Oliveira, *Refrigeração e cadeia do frio para alimentos*, Universidade de São Paulo, Faculdade de Zootecnia e Engenharia de Alimentos, Pirassununga, 2020.

48 S. Damodaran, K. L. Parkin and O. R. Fennema, *Química de alimentos de Fennema*, Artmed, 2010.

49 S. O. Adio, M. H. Omar, M. Asif and T. A. Saleh, *Process Saf. Environ. Prot.*, 2017, **107**, 518–527.

50 W. F. W. M. Nowalid, H. A. Hamid and S. H. Giwa, *Food Chem.: Mol. Sci.*, 2024, **8**, 100196.

51 H. Karazhiyan, S. M. A. Razavi and G. O. Phillips, *Food Hydrocolloids*, 2011, **25**, 915–920.

52 R. Rahmani and R. Firouzi, *Int. J. Commun. Network. Distr. Syst.*, 2021, **26**, 1.